Reciprocal irreversibility compensation of $LiNi_{0.2}Co_{0.2}Al_{0.1}Mn_{0.45}O_2$ cathode and silicon oxide anode in new Li-ion battery

Luca Minnetti[a], Vittorio Marangon[b,c], Paolo Andreotti[c], Antunes Staffolani[a], Francesco Nobili[a,*], and Jusef Hassoun[b,c,d*]

[a] *School of Sciences and Technologies – Chemistry Division, University of Camerino, Via Madonna delle Carceri ChIP, 62032, Camerino, Italy.*

[b] *Graphene Labs, Istituto Italiano di Tecnologia, via Morego 30, Genoa, 16163, Italy.*

[c] *Department of Chemical, Pharmaceutical and Agricultural Sciences, University of Ferrara, Via Fossato di Mortara 17, 44121, Ferrara, Italy.*

[d] *National Interuniversity Consortium of Materials Science and Technology (INSTM) University of Ferrara Research Unit, University of Ferrara, Via Fossato di Mortara, 17, 44121, Ferrara, Italy.*

*Corresponding authors: francesco.nobili@unicam.it, jusef.hassoun@unife.it

Supplementary Material

Figure S1 shows the EDS spectrum of LNCAM1000_12h collected to evaluate the sample stoichiometry, which is reported in Table 1 of the manuscript. The results confirm in a first approximation the stoichiometry expected by the theoretical formula $LiNi_{0.2}Co_{0.2}Al_{0.1}Mn_{0.45}O_2$, with molar ratio of 0.18, 0.2, 0.09 and 0.43 for Ni, Co, Al and Mn, respectively.

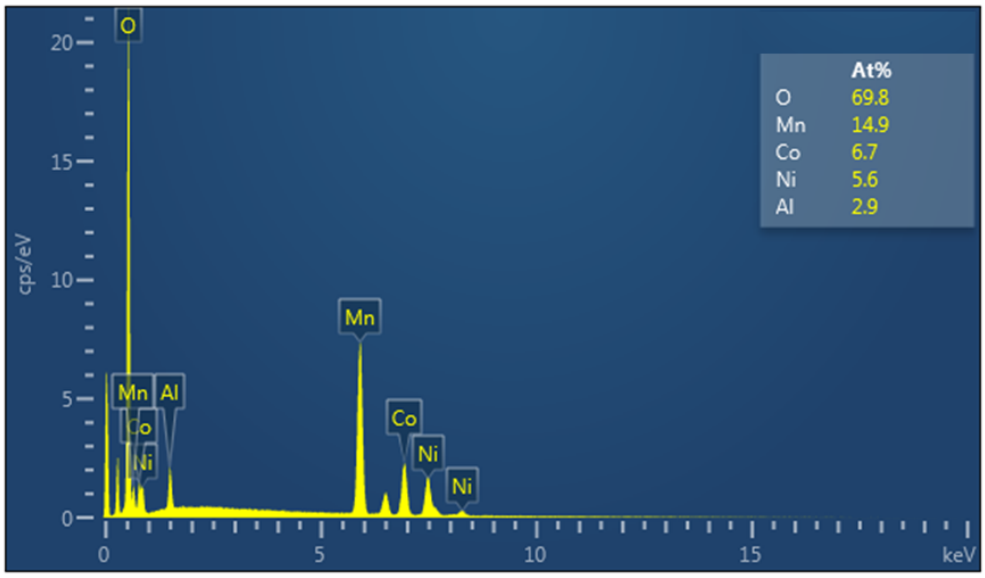

Figure S1. EDS spectrum of the LNCAM1000_12h material. Inset shows atomic percent composition. See Experimental Section in the Manuscript for acronyms.

Figure S2 reports the XRD patterns of the LNCAM500, LNCAM1000_6h and LNCAM1000_12h materials. The reference diffractogram of $LiNi_{0.4}Co_{0.15}Al_{0.05}Mn_{0.4}O_2$ (ICSD #166715) allows the indexing of the most relevant peaks [1]. The XRD patterns reveal broad and asymmetric peaks for the LNCAM500 precursor that tighten and become more defined upon treatment at 1000 °C with the formation of the LNCAM1000_6h sample. Thus, the final LNCAM1000_12h cathode material shows a well-defined (003) main reflection at 2θ = 18.72° as well as the (101), (006), (012), (104), (018), and (110) planes at 2θ = 36.67°, 37.82°, 38.32°, 44.46°, 64.48°, and 65.44°, respectively, characteristic of the P3-type layered oxide structure [2].

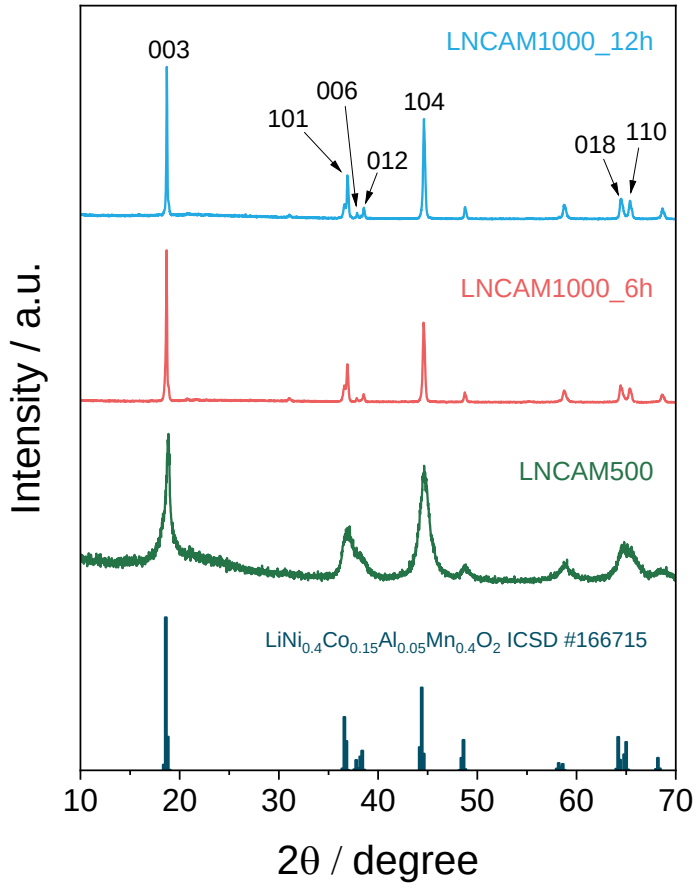

Figure S2. XRD patterns of the LNCAM500, LNCAM1000_6h, and LNCAM1000_12h materials, reference data of $LiNi_{0.4}Co_{0.15}Al_{0.05}Mn_{0.4}O_2$ (ICSD #166715) are reported for comparison and peaks indexing [1]. See Experimental section in the Manuscript for acronyms.

Figure S3 shows the LSV measurment performed on the Li| EC:DMC 1:1 v/v 1 M $LiPF_6$|SPC-Al cell used for determining the anodic electrochemical stability of the electrolyte. The LSV shows a small increase of the current around 5 V vs. Li^+/Li, while the full oxidative decomposition of the electrolyte was detected only at around 5.2 V vs. Li^+/Li. The obtained result is in agreement with various literature reports [3–5], and confirms the stability of the electrolyte for the study in lithium cell of the layered cathode within the voltage ranges used in this work.

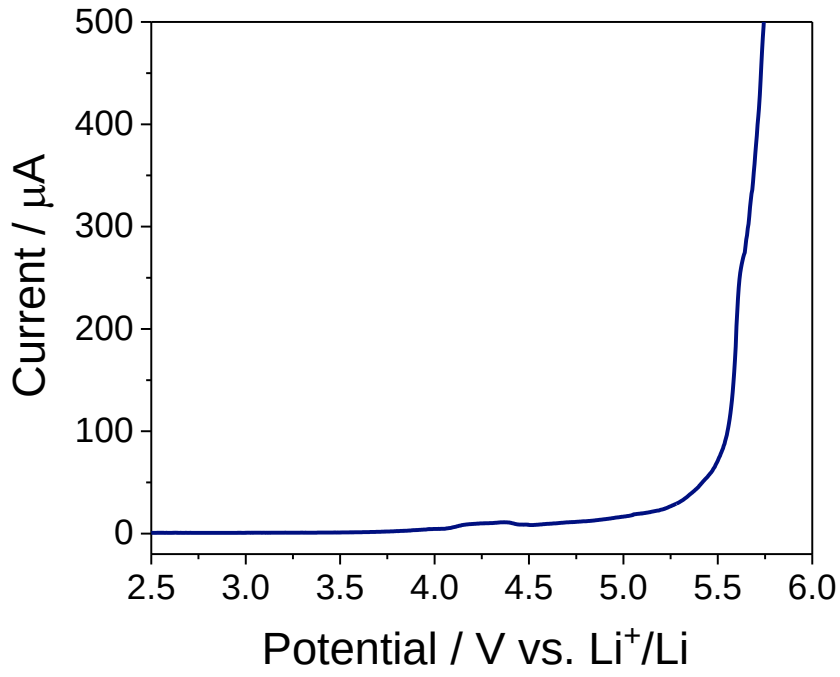

Figure S3. Linear sweep voltammetry (LSV) of the Li| EC:DMC 1:1 v/v 1 M $LiPF_6$|SPC-Al cell for determining the anodic electrochemical stability of the electrolyte. Scan rate 0.1 mV s^{-1}. See Experimental section in the Manuscript for acronyms.

Figure S4 displays the rate capability test of the LNCAM1000_12h electrode in lithium cell performed by increasing the current rate from C/10 to 1C (1C = 298 mA g^{-1}) in terms of the selected voltage profiles (Figure S4a) and capacity trend (Figure S4b). The voltage profiles in Figure S4a show the expected sloped behavior and limited polarization of the (de)intercalation process, which increases by current rate increment. The cell delivers reversible capacities of about 117, 109, 96, 80, and 46 mAh g^{-1} at C/10, C/8, C/5, C/3, and 1C, respectively, recovering a capacity of about 110 mAh g^{-1} when the C-rate is decreased back to C/10 after the 25th cycle (Figure S4b), thus suggesting moderate rate capability and stability of the layered oxide cathode [6].

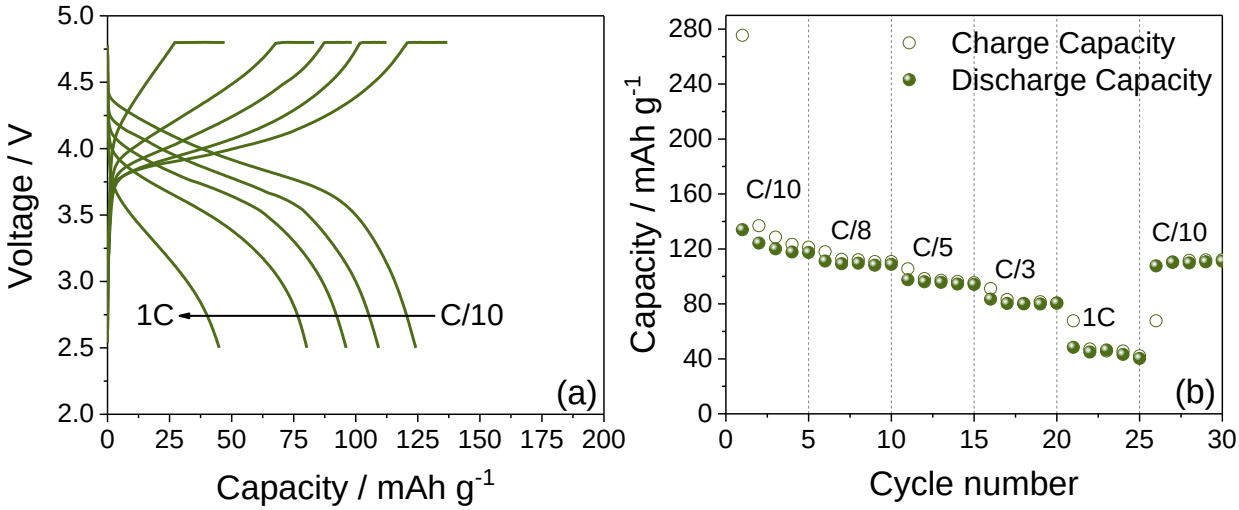

Figure S4. Rate capability test carried out on a Li|LNCAM1000_12h cell in terms of **(a)** voltage profiles and **(b)** corresponding cycling trend by using C/10, C/8, C/5, C/3 and 1C rates (1C = 298 mA g^{-1}). Voltage range: 2.5 – 4.8 V. Measurement performed with an additional constant voltage step at 4.8 V held until a current value of ¼ of the initial C-rate was reached (CCCV mode). Room temperature: 25 °C. See the Experimental section for acronyms.

Figure S5 reports the TGA measurement carried out on the carbon-coated silicon oxide (SiO_x-C) anode to evaluate the silicon/carbon ratio of the material. The figure shows an initial weight loss at about 150 °C ascribed to the evaporation of adsorbed water in the sample, and a second weight loss ranging from 500 to 780 °C related to carbon oxidation and CO_2 formation. The test reveals a residual of about 25% in weight, which is mainly composed by SiO_2, and a carbon content of about 70%, in agreement with data obtained in a previous paper [7].

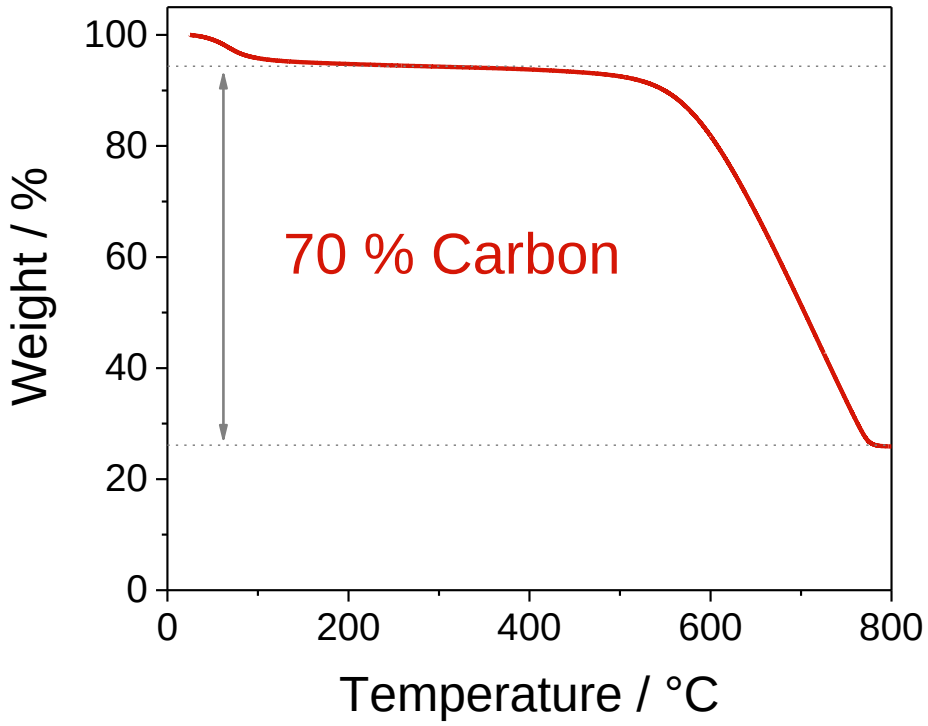

Figure S5. TGA curve of SiO_x-C recorded under air flow in the 25 – 800 °C temperature range at a heating rate of 5 °C min^{-1}, reporting the obtained carbon weight %. See the Experimental section for acronyms.

Figure S6 depicts the cycling behavior of the full SiO_x-C|LNCAM1000_12h coin-type cell in terms of cycling trend, prolonged to 50 charge/discharge cycles, delivered at C/10 with N/P ratio of 0.91. The cell shows high irreversible charge capacity at the first cycle, that is 294 mAh g^{-1}, and discharge capacity of 104 mAh g^{-1}, with corresponding coulombic efficiency of 35%. Subsequently, the cell delivers a capacity of about 80 mAh g^{-1} after initial cycles, stabilized at about 70 mAh g^{-1} after 20 cycles and retained until the end of the test, with a coulombic efficiency approaching 85%. These data confirm the need of further optimization of the electrode balancing to achieve higher cell capacity [8].

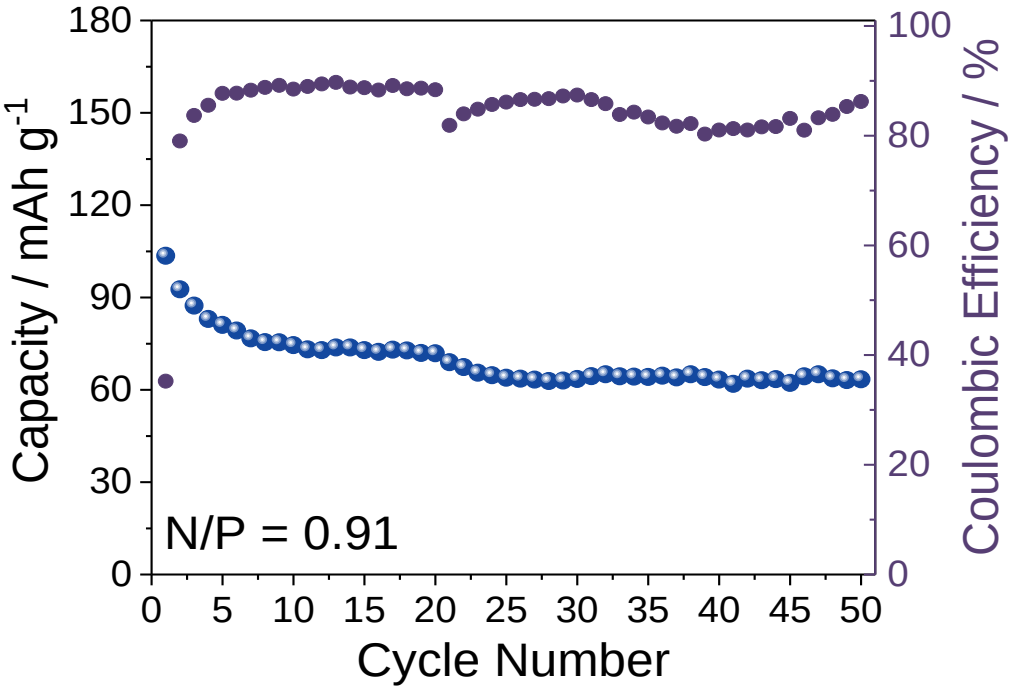

Figure S6. Capacity trend (right *y*-axis show coulombic efficiency) of the SiO_x-C|EC:DMC 1:1 v/v 1 M $LiPF_6$|LNCAM1000_12h full cell with N/P ratio of 0.91 cycled at the constant current rate of C/10 (1C = 298 mA g^{-1}). Voltage range: 1.5 – 4.8 V. Measurements performed with an additional constant voltage step at 4.8 V held until a current value of ¼ of the nominal C-rate was reached (CCCV mode). Room temperature (25 °C). See the Experimental section for acronyms.

References

[1] J.D. Wilcox, E.E. Rodriguez, M.M. Doeff, The Impact of Aluminum and Iron Substitution on the Structure and Electrochemistry of $Li(Ni_{0.4}Co_{0.2-y}M_yMn_{0.4})O_2$ Materials, J Electrochem Soc. 156 (2009) A1011. https://doi.org/10.1149/1.3237100.

[2] K.S. Park, M.H. Cho, S.J. Jin, K.S. Nahm, Y.S. Hong, Effect of Li ion in transition metal sites on electrochemical behavior of layered lithium manganese oxides solid solutions, Solid State Ionics. 171 (2004) 141–146. https://doi.org/10.1016/j.ssi.2004.04.016.

[3] J. Demeaux, M. Caillon-Caravanier, H. Galiano, D. Lemordant, B. Claude-Montigny, $LiNi_{0.4}Mn_{1.6}O_4$/Electrolyte and Carbon Black/Electrolyte High Voltage Interfaces: To Evidence the Chemical and Electronic Contributions of the Solvent on the Cathode-

Electrolyte Interface Formation, J Electrochem Soc. 159 (2012) A1880–A1890. https://doi.org/10.1149/2.052211jes.

[4] V. Sharova, A. Moretti, T. Diemant, A. Varzi, R.J. Behm, S. Passerini, Comparative study of imide-based Li salts as electrolyte additives for Li-ion batteries, J Power Sources. 375 (2018) 43–52. https://doi.org/10.1016/j.jpowsour.2017.11.045.

[5] J. Kasnatscheew, B. Streipert, S. Röser, R. Wagner, I. Cekic Laskovic, M. Winter, Determining oxidative stability of battery electrolytes: validity of common electrochemical stability window (ESW) data and alternative strategies, Physical Chemistry Chemical Physics. 19 (2017) 16078–16086. https://doi.org/10.1039/C7CP03072J.

[6] M. Zukalova, J. Prochazka, B. Pitna Laskova, A. Zukal, L. Kavan, Layered $LiNi_{1/3}Mn_{1/3}Co_{1/3}O_2$ (NMC) with Optimized Morphology for Li-Ion Batteries, ECS Trans. 87 (2018) 67–75. https://doi.org/10.1149/08701.0067ecst.

[7] G.A. Elia, J. Hassoun, A SiO_x-Based Anode in a High-Voltage Lithium-Ion Battery, ChemElectroChem. 4 (2017) 2164–2168. https://doi.org/10.1002/celc.201700316.

[8] Ahmed.M. Hashem, Rasha.S. El-Tawil, M. Abutabl, Ali.E. Eid, Pristine and coated $LiNi_{1/3}Mn_{1/3}Co_{1/3}O_2$ as positive electrode materials for li-ion batteries, Research on Engineering Structures & Materials. 1 (2015) 81–97. https://doi.org/10.17515/resm2015.07en0315.